



**HAL**  
open science

## Integrated symmetrical organic/semiconductor structures produced by hybrid processes: photonic micro-resonators cavities

Rémi Sevestre, Nathalie Coulon, Lucas Garnier, Alain Moréac, Hervé Cormerais, Laurent Le Brizoual, France Le Bihan, Didier Balcon, Bruno Bêche

### ► To cite this version:

Rémi Sevestre, Nathalie Coulon, Lucas Garnier, Alain Moréac, Hervé Cormerais, et al.. Integrated symmetrical organic/semiconductor structures produced by hybrid processes: photonic micro-resonators cavities. Proceedings of SPIE, the International Society for Optical Engineering, 2022, Organic Electronics and Photonics: Fundamentals and Devices, 12149, pp.1214907.1-1214907.7. 10.1117/12.2617999 . hal-03667408

**HAL Id: hal-03667408**

**<https://hal.science/hal-03667408>**

Submitted on 31 May 2022

**HAL** is a multi-disciplinary open access archive for the deposit and dissemination of scientific research documents, whether they are published or not. The documents may come from teaching and research institutions in France or abroad, or from public or private research centers.

L'archive ouverte pluridisciplinaire **HAL**, est destinée au dépôt et à la diffusion de documents scientifiques de niveau recherche, publiés ou non, émanant des établissements d'enseignement et de recherche français ou étrangers, des laboratoires publics ou privés.

# Integrated symmetrical organic/semiconductor structures produced by hybrid processes: photonic micro-resonators cavities

R. Sevestre<sup>a</sup>, N. Coulon<sup>a</sup>, L. Garnier<sup>a</sup>, H. Lhermite<sup>a</sup>, A. Moréac<sup>b</sup>, H. Cormerais<sup>a,c</sup>,  
L. Le Brizoual<sup>a</sup>, F. Le Bihan<sup>a</sup>, D. Balcon<sup>a</sup>, B. Bêche<sup>\*a</sup>

<sup>a</sup>Université de Rennes, CNRS, Institut d'Électronique et des Technologies du numÉrique - IETR UMR 6164 F-35000 Rennes, France; <sup>b</sup>Université de Rennes 1, CNRS, Institut de Physique de Rennes - IPR UMR 6251, F-35000 Rennes, France; <sup>c</sup>Centrale/Supelec, Campus de Rennes, F-35510 Cesson-Sévigné, France

\*[bruno.beche@univ-rennes1.fr](mailto:bruno.beche@univ-rennes1.fr); <https://www.ietr.fr/bruno-beche>

## ABSTRACT

In this study we are interested in the implementation of mixed processes for the realization of symmetrical structures shaped in thin layers for integrated photonics and based on silicon plus organic UV210. We used the so called UV210 polymer for shaping the core waveguide. The UV210 polymer made up of poly (p-hydroxystyrene) and poly (t-butyl acrylate) is a chemically amplified resin; a photo-acid generator is added to the matrix of the copolymer in order to increase the sensitivity of the resin and create a chain reaction during developments so as to develop sub-wavelength patterns. Several families of multilayers structures have been produced by specific sub-wavelength lithography plus PECVD, and then properly characterized by including stoichiometry analyses plus imaging by Raman. The advantage of achieving Si/SiO<sub>2</sub>/UV210/Si/SiO<sub>2</sub> symmetry relates first of all to the equations of electromagnetism and guidance which no longer impose a cut-off thickness (or frequency) during extreme miniaturization, but also for an adequate protection of the components by an upper layer of silicon covering the surface of the chip for sensor applications and specific detection of aggressive substances / agents. All structures, including the addition of silicon directly onto the organic, exhibit excellent mechanical strength and optical stability; the last silicon/silica bilayer also acts as a thin protective shell. Various families of resonant photonic structures could be cleanly characterized on platform. Furthermore, by statistical measurements of resonance parameters, we conclude that the processes and properties of the materials obtained have good reproducibility. This opens the way to the realization of sensors dedicated to aggressive substances directly in contact with the resonant elements probing it.

**Keywords:** Integrated photonics, organic UV210 and silicon on insulator (SOI), Raman analyzes, resonators cavities, optical characterizations, sensors.

## 1. INTRODUCTION

In integrated photonics<sup>1,2</sup> and more generally in electromagnetism and propagation<sup>3</sup>, the calculation of solutions concerning mathematical modes can be reduced to a problem with eigenvalues and eigenvectors to be solved for complex and varied structures. When classes of mathematical solutions exist in the form of guided modes, leaky and radiated modes, their relevant eigenvalues represent so-called effective propagation constants  $\beta = k_0 \cdot n_{\text{eff}} = (2\pi/\lambda_0) \cdot n_{\text{eff}}$  or even in photonics their effective indices  $n_{\text{eff}}$  which takes into account electromagnetic radiation (light in optics) in the whole system or overall photonic structure. These last eigenvalues are related to the wave vector  $k_0 = 2\pi/\lambda_0$  and the wavelength  $\lambda_0$  in wave physics (J.C. Maxwell). In integrated photonics, such eigenvalues are solutions of opto-geometric equations called eigenvalue equations; each eigenvalue can be associated with an unfolded mode in the complete structure; its specific spatial distribution represents the optical intensity or the modulus of the field. A particularity of pure symmetric systems is that they do not have cut-off thicknesses or cut-off frequencies and can thus ensure electromagnetic propagation with extremely low characteristic thicknesses<sup>4,5</sup>. On this strategy, technological processes have been developed in recent decades to achieve successfully symmetrical integrated photonic structures SiO<sub>2</sub>/Si/SiO<sub>2</sub>

or Semiconductors On Insulator (SOI)<sup>6-10</sup>. The control of these processes on the thickness of the successively deposited layers has moreover made it possible to produce single-mode nanostructures with low losses and even independent of the state of polarization for telecommunications applications. At the same time, in recent years new specific resins flashing in deep UV have participated in the production of nano-waveguides and sub-micrometer patterns such as gaps between guides<sup>11-12</sup>. In the context of producing components as resonators type<sup>13</sup>, such organics and resins, which develop relatively easily for the shaping of 200 nm patterns, have influenced the development of organic resonators dedicated to specific sensor applications. The detection of chemical and biological species was thus carried out with great precision and sensitivity<sup>14-16</sup>. Moreover other applications such as phase transition measurements in biology, cosmetics and the food industry<sup>17-18</sup> have also emerged in metrology<sup>19</sup>. However, despite their flexible shaping and low cost, organic resonators will not always be able to probe highly aggressive substances for certain targeted energy applications. It will then be necessary to shell them with a hard top coat.

The purpose of the paper is to study a possible transfer of the principle of realization of hybrid symmetric structures in Semiconductors On Insulator based on an Organic<sup>11</sup> (SOI with Org.). The structures SOI with Org. made by these hybrid processes will be composed of waveguides, tapers and micro-resonators (MRs). Thus, the first part will be dedicated to the description of all the technology processes that have allowed the realization of such symmetrical arrangements of hybrid materials SOI with Org. Various analyzes and imaging, including Raman, will validate and clarify the shape and composition of the multilayers produced and shaped. Finally, a second part will be devoted to the presentation of experimental measurements and results in terms of injection and guided propagation; in particular the final test of resonator type components integrated on SOI with Org will be presented.

## 2. MATERIALS AND PROCESSES

### 2.1 Design

The design of the masks was established by software creating all the integrated photonic structures, namely, guides, tapers, resonators and so on. The 4 inch masks are then created on quartz/metal, the organic DUV 210 flashing at 248 nm. Figure 1 shows by way of example the type of structures drawn on software in the appropriate format.

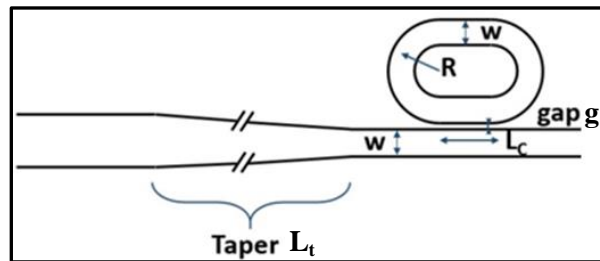


Figure 1. Diagram of a set of plane guide structure, taper, monomode rib guide coupled to a resonator. The parameters  $L_t$ ,  $w$ ,  $L_c$ ,  $R$  and  $g$  respectively represent the length of the taper of 100  $\mu\text{m}$ , the width of a guide of 3  $\mu\text{m}$ , a coupling length then a radius of 5  $\mu\text{m}$  and a gap of 0.4  $\mu\text{m}$ .

### 2.2 Fabrication procedures and materials

On a silicon substrate, a thermal silica layer is formed by wet oxidation method. We must first clean the wafer with the method RCA (developed by 'Radio Company of America'), to avoid all impurities. The plate is then put in a quartz oven with torch, the gas  $\text{H}_2$  and oxidation gas  $\text{O}_2$  being located in the flame for the combustion. A typical 4h hours stage in the oven at 1175°C can form 1.6  $\mu\text{m}$  of silica on the surface of the wafer, creating the silica lower cladding. After oxidation, the annealing at 700°C-800°C strengthens the single crystal structure. Such a thickness guarantees a highly stable and homogeneous refractive index under the organic waveguides and MRs so as to decrease the optical radiation losses regarding the propagation modes. After the substrate/cladding manufacturing, organic patterns are grown and shaped by way of specific processes involving deep UV lithography suited to the DUV210 polymer which is an amplified chemical resist. Such a deep UV (DUV) polymer made of poly p-hydroxystyrene and poly t-butyl acrylate is called an amplified chemical photoresist because it includes a photo acid generator (PAG) to increase the sensitivity with UV energy exposure as regards such a specific photolithography mechanism. Indeed the DUV-insolation induces the

production with the PAG of a small quantity of acid acting as a catalyst during the exposure. Thermally activating this acid with a post exposure bake causes the proton H<sup>+</sup> to act as a catalyst and unblock the group from the PHS. Then, the cascade of acid activated chemical changes brings about a change in polarity of the polymer which goes from lipophilic to hydrophilic states. This make the PHS soluble in the exposed areas. Thus, DUV exposed areas become soluble in a basic developer as the tetra-methyl ammonium hydroxide. Relevant integrated DUV210 MRs photonics structures have been fabricated according to such simple procedures. The adequate and global optimized processes are illustrated in the following Table 1.

Table 1. Processes for the fabrication of symmetrical Si/SiO<sub>2</sub>/UV210/Si/SiO<sub>2</sub> photonic resonators and circuits.

<b>Thermal oxidation (SiO<sub>2</sub> into Si)</b>	<b>Parameters</b>
Humid pyrolitic oxidation (AET Technologies)	4h35min at 1175°C <ul style="list-style-type: none"> <li>- i) O<sub>2</sub> (2 l/min) + N<sub>2</sub> (2 l/min) 5 min</li> <li>- ii) O<sub>2</sub> (2 l/min) 10 min</li> <li>- iii) H<sub>2</sub> (1.8 l/min) + O<sub>2</sub> (1 l/min) 4 h</li> <li>- iv) N<sub>2</sub> (2 l/min) 20 min</li> </ul>
<b>Photolithography procedure /steps (Organic UV210)</b>	<b>Parameters</b>
Spin-coating (v,a,t), thickness, roughness Softbake Deep UV exposure + Post-exposure soft-bake Development + Final softbake	(900 rpm, 5000rpm/s, 30s), ~800-850 nm, <3 nm 3 min at 140°C E = 20 mJ/cm <sup>2</sup> during 27 s + 1 min at 120°C 30 s, with Microposit MF CD-26 + 24 h at 120°C
<b>PECVD (Si and SiO<sub>2</sub>)</b>	<b>Parameters</b>
Plasma enhanced chemical vapor deposition Substrate temperature 150 °C and 120°C Silane gas or silane plus nitrous oxide gas	Time depending of the thicknesses (10 nm/min < deposition rates < 50 nm/min) <ul style="list-style-type: none"> <li>- i) SiH<sub>4</sub>, 10 sccm, , 0.16 mbar at 12 W</li> <li>- ii) SiH<sub>4</sub> and N<sub>2</sub>O, 0.90 mbar at 15W</li> </ul>

A baking step makes the surplus solvent to evaporate and strengthens the adhesion of the polymer onto silica. The deep UV exposure is performed with a mercury short arc lamp (HBO 1000W/D, OSRAM). The previous quartz chromium mask is arranged above the wafer with the spread polymer layer. The lithographic pattern to be transferred is printed onto the mask and a 30 seconds exposure duplicates the mask patterns on the wafer in a suitable way. Moreover, a post-exposure soft-bake of 1 min annealing at 120 °C promotes the polymerization reaction so as to minimize the surface roughness (< 2 nm). Then, immersion in the developer Microposit MF CD-26 allows us to get the whole chip featuring all the elements as MRs. Finally, with the aim of protecting the resonator elements (for sensor applications of aggressive substances) but also with the aim of developing the know-how and the ability to create symmetrical hybrid structures SOI with Org. a two-step PECVD type deposition has been developed. Three types of bilayers/shells (and therefore of complete structures) have been produced to protect the resonators and to create such Si/SiO<sub>2</sub>/UV210/Si/SiO<sub>2</sub> multilayers for photonics. For the first kind of structure, only a first PECVD using silane gas at a substrate temperature of 150°C was used to create Si layer. For the other two kinds of structures, two PECVDs, that consist of both successive steps so as to create Si/SiO<sub>2</sub> above the guides and the organic resonators have been employed by respectively a flow of silane gas (SiH<sub>4</sub>) then by a mixture of silane and nitrous oxide (SiH<sub>4</sub> and N<sub>2</sub>O). Such second stage of the PECVD was carried out at a substrate temperature of 120° C and 150° C for respectively the second and third type of complete structure considered. Typically with these PECVD parameters, the deposition rates are respectively 10 nm per min for silicon and 50 nm per min for silica. At the end of the process, it is a bi-layer between 5 and 10 nm of silicon which is deposited on the photonic structures plus typically 20 nm of silica.

Table 2. Types of heterostructures and differentiating parameters regarding substrate temperature during PECVD.

SOI with Org. heterostructures 'Si/SiO <sub>2</sub> /UV210/Si/SiO <sub>2</sub> '	PECVD Parameters of the upper cladding
<b>Type I</b>	<b>T=150°C - Amorphous Si :</b> SiH <sub>4</sub> , 10 sccm, , 0.16 mbar at 12 W
<b>Type II</b>	<b>T=120°C - Amorphous Si :</b> SiH <sub>4</sub> , 10 sccm, , 0.16 mbar at 12 W <b>T=120°C - SiO<sub>2</sub> :</b> SiH <sub>4</sub> and N <sub>2</sub> O, 0.90 mbar at 15W
<b>Type III</b>	<b>T=120°C - Amorphous Si :</b> SiH <sub>4</sub> , 10 sccm, , 0.16 mbar at 12 W <b>T=150°C - SiO<sub>2</sub> :</b> SiH <sub>4</sub> and N <sub>2</sub> O, 0.90 mbar at 15W

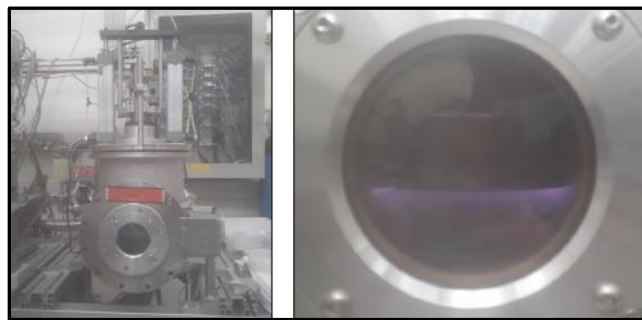


Figure 2. Vacuum plasma chamber (built by the team, <https://www.ietr.fr/equipe-oasis-organic-and-silicon-systems>) where the wafers are deposited between two electrodes for SOI deposits as upper cladding.

Such a Si/SiO<sub>2</sub> bilayer, making symmetrical photonic structures of the SOI type with Org. is also sufficient to stabilize and harden the resistance of the component in contact with aggressive substances to be studied (sensor applications).

### 2.3 Optical and Raman analysis, imaging

Figure 3 represents an optical imaging by microscopy, first of all as the cross-sectional view of SOI with Org. guide (Si/SiO<sub>2</sub>/UV210/Si/SiO<sub>2</sub>), then from above a view of the plane structures, tapers, ribs and resonators. All the processes reported in Table 1 allowed such optimal realization of symmetrical structures for photonics.

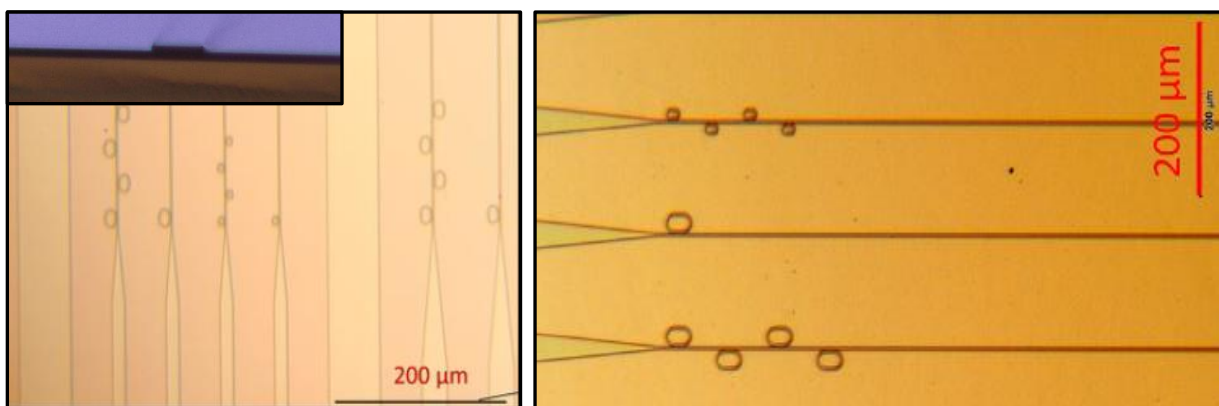


Figure 3. Optical microscopy of the symmetrical hybrid structures produced: cross-sectional and top views.

Due to the 2D-planar geometry of the photonics structures, Raman spectroscopy is performed assuming a two dimensional analysis with the LabRAM HR800 Raman Spectrometer (from Horiba Scientific company, Jobin-Yvon); this is a high resolution spectral spectrometer coupled with a confocal microscope, several laser sources (633 nm He-Ne), (785 nm Toptica) and (532 nm Coherent) and nano-positioners. The coupling with a confocal microscope enables us to imaging a sample in 2D with a spatial resolution of the order of the spot size ( $0.9 \mu\text{m}$ ) in the focal plane and a spectral resolution of typically  $1 \text{ cm}^{-1}$  per pixel. An apt laser excitation power lower than  $0.1 \text{ mW}$  is devoid of heating effect onto the photonics chip. The studies by micro-Raman vibrational molecular spectroscopy and analysis measurements without destruction of materials, were carried out and results recorded on a LabRAM HR 800 used in visible configuration. Then it is possible to select an area of the structure to analyze over the wafer or in the cut section too (see Figure 4, cross-sectional view of the rib heterostructure).

The micro-Raman spectroscopy analyses and detection of various signal signatures of each micro-material Si, UV210, can be led and the specific complex signal established and analyzed : for example the stretching mode of phenyl ring at  $1002 \text{ cm}^{-1}$  and the bending mode of aromatic olefinic at  $850 \text{ cm}^{-1}$  for the organic UV210. The peaks of the organic UV210 have for example emerged from the complete signal by filtering/decorrelation, so as to remove the residual fluorescence background (Figure 4). Depending on the selected area to analyze, we also note very clearly first of all the peak ( $1^{\text{st}}$  order) of the crystalline silicon<sup>20</sup> due to the wafer around  $521 \text{ cm}^{-1}$  and just before a wider peak specific to the amorphous silicon<sup>20</sup> which proved to be deposited by the PECVD (Figure 4).

It can be noted that the Raman signal specific to silica ( $\text{SiO}_2$ ) is extremely weak (not visible) and extended towards low frequencies<sup>21</sup> (main band from  $200 \text{ cm}^{-1}$  up to  $400 \text{ cm}^{-1}$ ) compared to the signals of silicon and the organic UV210 which interest us. Moreover, filtering the enlarged signature and then choosing specific peaks characterizing the various materials Si, UV210, it is also possible to image on 2D the various waveguide/MR structures for a stringent quality control on geometry and materials.

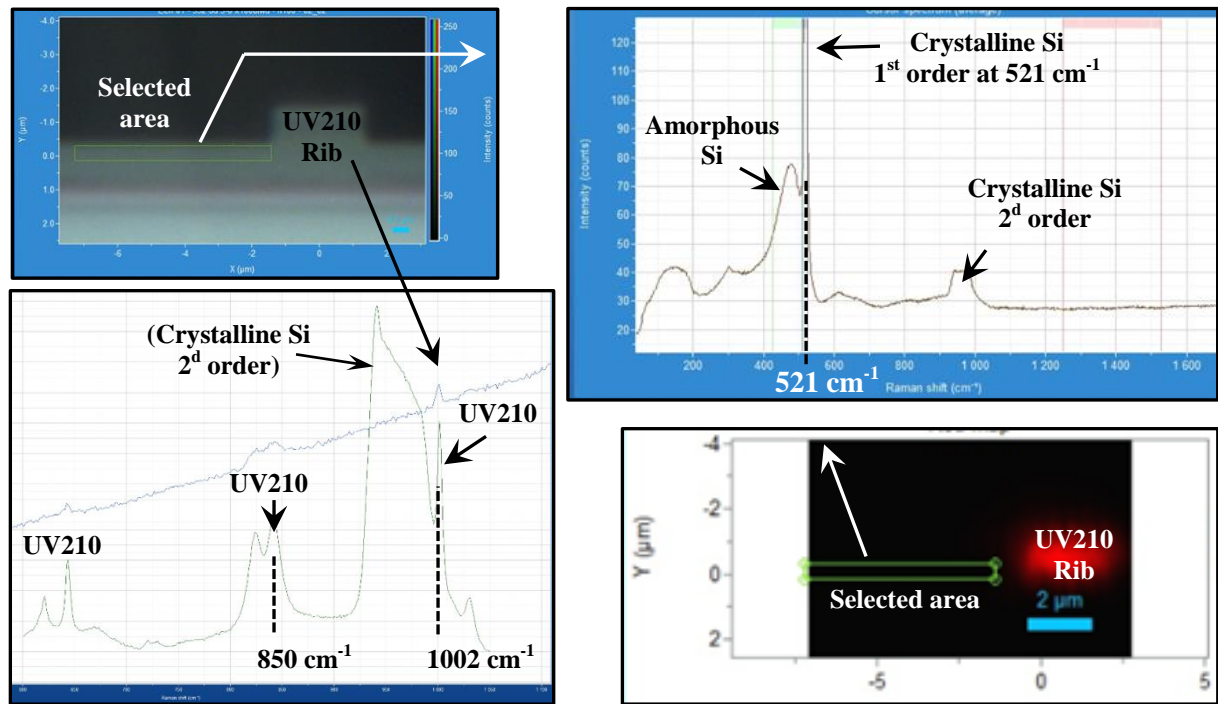


Figure 4. Raman analyzes of SOI ( $\text{Si}/\text{SiO}_2$ ) symmetric structures with Org. (UV210) performed. The peaks of crystalline Si (wafer) then Si amorphous (upper cladding) as well as those of organic UV210 have been clearly identified.

### 3. EXPERIMENTAL RESULTS, DISCUSSIONS AND CONCLUSION

Such ( $\text{Si}/\text{SiO}_2/\text{UV210}/\text{Si}/\text{SiO}_2$ ) photonic heterostructures and micro-resonators are based on a coupling and resonance physics, with a tunnel effect through a gap added with an optical geometric and cyclic resonance. The quantifications

localize into the resonator emerge due to the installation of a cyclic condition (or stationary waves) written as  $P_{\text{opt}} = t \cdot \lambda$ , with  $P_{\text{opt}}$  the ‘optical’-perimeter of the micro-resonator,  $\lambda$  the optical wavelength of the light and  $t$  an integer. Quantifications can be measured by tracking the pseudo-period or Free Spectral Range (FSR) of the transduced spectra. Indeed, the FSR verifies  $\text{FSR} = \frac{\lambda_0^2}{P \cdot n_{\text{eff}}^2} = \frac{\lambda_0^2}{P_{\text{opt}}}$ , with  $\lambda_0$  the central excitation wavelength and  $P$  the geometrical perimeter of the resonator.

### 3.1 Experimental measurements and results

A broadband source is used to highlight and create relevant quantified resonant modes. A single mode fiber is connected to the laser source (SUPERLUM, SLD 331 HP3,  $\lambda_0=795$  nm and 40 nm spectrum width) and a lens system is arranged to focus the incident beam and achieve this type of photonic micro-injection. A polarizer secures the polarization state, TE or TM. The supports are controlled with nano-piezoelectric actuators (PI-563I.3 E) with a  $\pm 10$  nm pitch in the three spatial dimensions. Such handlings and other specific injection protocols are used to excite and measure the quantified resonances. A third lens is positioned to recover the output light for respectively a CCD camera (Imaging Source, control the single-mode video characteristic) and into single-mode fiber to be sent to the Spectrum Analyzer Optical (OSA Ando AQ-6315E) or spectrometer (HR 4000, Ocean Optic).

Figure 5 represents the resonance spectrum of a heterostructure family III, ‘Si/SiO<sub>2</sub>/UV210/Si/SiO<sub>2</sub>’ type, with an upper cladding deposited by PECVD (amorphous Si at a 120°C substrate temperature and SiO<sub>2</sub> at 150°C). On the right, Figure 5 represents a statistic on twenty spectra of the measurements of the pseudo period FSR measured on each type I, II and III of heterostructures.

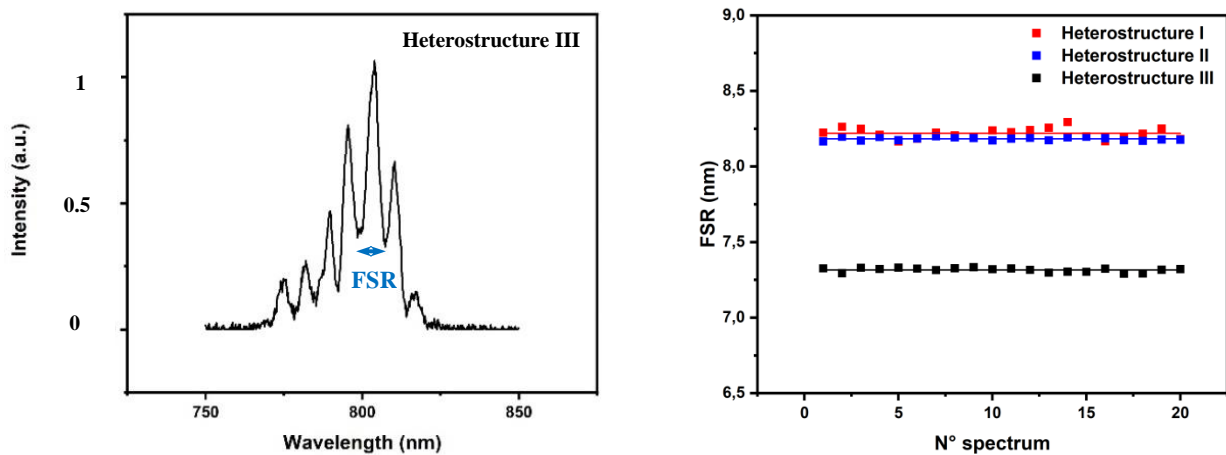


Figure 5. On the left, an example of resonant quantified spectrum specific to the family of heterostructures III; the FSR represents the pseudo period of the spectrum which is close to 7.31 nm. On the right, the statistical measurements of the spectra of the three various families I, II and III of structures produced.

### 3.2 Discussions and conclusions

One can notice that the third heterostructure presents a smaller FSR which means that the resonant mode located in the resonator presents a stronger effective group index (eigenvalue); this is probably due to the last silica deposit by PECVD at higher temperature.

All of these hybrid processes of thermal oxidation, photolithography on organic UV210 followed by PECVD have enabled us to be able to reproducibly produce these types of symmetrical heterostructures SOI with Org. In addition to having validated the production of series of guides, tapers and micro-resonators, the precise and very fine principle of physic resonances (furthermore by repetitive statistical measurements of the FSRs) thus indicated a very good reproducibility of the qualities of the layers deposited onto each of the families of heterostructures.

**Acknowledgments:** The authors would like to thank the ‘Société d’Accélération du Transfert de Technologies’ (SATT Ouest Valorisation), the NanoRennes Plateforme (<https://www.ietr.fr/plateforme-nr-nanorennnes>) and the Scan Mat service unit (<https://scanmat.univ-rennes1.fr/>, including Raman) for financially and help supporting this research. This study is also a part of a PASS\_programm ‘cordée de la réussite’ named ‘Pour une Ambition Scolaire Scientifique’ (For a Scientific School Ambition) with the Brittany center (Sir Cyril Le-Corre and Madame Valérie Mesnet at Lycée Fulgence Bienvenüe, and Collèges Louis Guilloux, Paul Eluard, Romain Rolland, <https://spm.univ-rennes1.fr/les-cordees-de-la-reussite>).

## REFERENCES

- [1] Adams, M.J., [Introduction to Optical Waveguides], John Wiley & Sons, New-York, (1981).
- [2] Snyder, A.W. and Love, J.D., [Optical Waveguide Theory], 2d ed. Kluwer Academic Publishers, (2000).
- [3] Collin, R.E., [Field Theory of Guided Waves], 2d ed. IEEE Press, New-York, (1991).
- [4] Duval D. and Bêche B., “Theoretical formulation to shape versatile propagation characteristics of three-layer-tubular waveguides: sub-wavelength and asymptotic study”, *IoP J. Opt.* 12, 075501.1-075501.10 (2010).
- [5] Bêche, B. and Gaviot, E., “About the Heisenberg’s uncertainty principle and the determination of effective optical indices in integrated photonics at high sub-wavelength regime”, *Optik* 127, 3643-3645 (2016).
- [6] Schmidtchen, J., Schüppert, B., Splett, A. and Petrmann, K., “Low loss rib-waveguides in SOI”, *Mat. Res. Soc. Symp. Proc.* 244, 351-355 (1992).
- [7] Vivien, L., Laval, S., Dumont, B., Lardenois, S., Koster, A. and Cassan, E., “Polarization-independent single-mode rib waveguides on silicon-on-insulator for telecommunication wavelengths”, *Opt. Comm.* 210, 43-49 (2002).
- [8] Angulo Barrios, C., Almeida, V.R., Panepucci, R. and Lipson, M., “Electrooptic modulation of silicon-on-insulator submicrometer-size waveguide devices”, *J. Lightwave Technol.* 21, 2332-2339 (2003).
- [9] Ye, W.N., Xu, D.X., Janz, S., Cheben, P., Delâge, A., Picard, M.J., Lamontagne, B. and Tarr, N.G., “Stress-induced birefringence in silicon-on-insulator (SOI) waveguides”, *Proc. SPIE* 5357, 57-66 (2004).
- [10] Passaro V.M.N., Magno, F. and Tsarev, A.V., “Investigation of thermos-optic effect and multi-reflector tunable filter/multiplexer in SOI waveguides”, *Opt. Express* 13, 3429-3437 (2005).
- [11] Rohm and Haas Electronic Materials, “UV 210 Positive photoresist”, April 2005, <https://kayakuam.com/products/uv-210gs-positive-duv-photoresist/> (Kayaku Advanced Materials, Inc.’s, 2021).
- [12] Duval, D., Lhermite, H., Godet, C., Huby, N. and Bêche, B. “Fabrication and optical characterization of sub-micronic waveguide structures on UV210 polymer”, *IoP J. Optics* 12, 055501/1-055501/6 (2010).
- [13] Rabus, D.G., [Integrated Ring Resonators: the Compendium], Springer-Verlag, New-York, (2007).
- [14] Chauvin, D., Bell, J., Leray, I., Ledoux-Rak, I. and Nguyen, C.T., “Label-free optifluidic sensor based on polymeric microresonator for the detection of cadmium ions in tap water”, *Sensors Actuators B* 280, 77-85 (2019).
- [15] Meziane, F., Raimbault, V., Hallil, H., Joly, S., Conédéra, V., Lachaud, J.L., Béchou, L., Rebière, D. and Dejous, C., “Study of a polymer optical microring resonator for hexavalent chromium sensing”, *Sensors Actuators B* 209, 1049-1056, (2015).
- [16] Castro Beltran, R., Huby, N., Vié, V., Lhermite, H., Camberlein, L., Gaviot, E. and Bêche, B., “A laterally coupled UV210 polymer racetrack micro-resonator for thermal tunability and glucose sensing capability”, *Adv. Dev. Mat.* 1, 80-87, (2015).
- [17] Li, Q., Vié, V., Lhermite, H., Gaviot, E., Moréac, A., Morineau, D., Bourlieu, C., Dupont, D., Beaufils, S. and Bêche, B., “Polymer resonators sensors for detection of sphingolipid gel/fluidphase transition and melting temperature measurement”, *Sensors Actuators Phys. A* 263, 707-717 (2017).
- [18] Castro Beltran, R., Garnier, L., St Jalmes, A., Lhermite, H., Gicquel, E., Cormerais, H., Fameau, A.L. and Bêche, B., “Microphotonics for monitoring the supramolecular thermoresponsive behavior of fatty acid surfactant solutions”, *Opt. Comm.* 468, 125773.1-7 (2020).
- [19] Garnier, L., Lhermite, H., Vié, V., Pin, O., Liddel, Q., Cormerais, H., Gaviot, E. and Bêche, B., “Monitoring the evaporation of a sessile water droplet by means of integrated resonator”, *IoP J. Phys. D: Appl. Phys.* 53, 125107.1-125107.10 (2020).
- [20] Hong, W.E. and Ro J.S., “Kinetics of solid phase crystallization of amorphous silicon analyzed by Raman spectroscopy”, *J. Appl. Phys.* 114, 073511.1-073511.6 (2013).
- [21] Degioanni, S., Jurdyc, A.M., Cheap, A., Champagnon, B., Bessueille, F., Coulm, J., Bois, L. and Vouagner, D., “Surface-enhanced Raman scattering famorphous silica gel adsorbed on old substrates for optical fiber sensors”, *J. Appl. Phys.* 118, 153103.1-153103.7 (2015).